

## Journal Pre-proofs

Research paper

Crystal structure and infrared and Raman spectra of  $K_3[Cr(CN)_5NO] \cdot 2H_2O$ , a member of an iconic family of complexes in coordination chemistry

Oscar E. Piro, Gustavo A. Echeverría, A. Navaza, Jorge A. Güida

PII: S0020-1693(20)31030-6  
DOI: <https://doi.org/10.1016/j.ica.2020.119831>  
Reference: ICA 119831

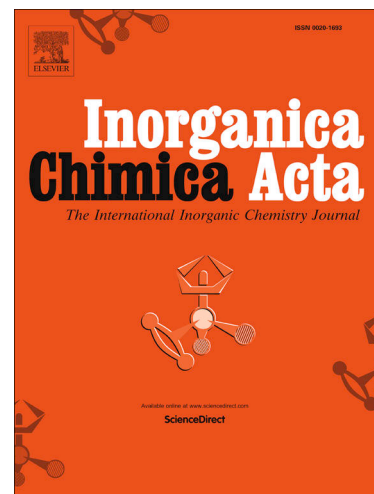
To appear in: *Inorganica Chimica Acta*

Received Date: 6 March 2020  
Revised Date: 8 June 2020  
Accepted Date: 10 June 2020

Please cite this article as: O.E. Piro, G.A. Echeverría, A. Navaza, J.A. Güida, Crystal structure and infrared and Raman spectra of  $K_3[Cr(CN)_5NO] \cdot 2H_2O$ , a member of an iconic family of complexes in coordination chemistry, *Inorganica Chimica Acta* (2020), doi: <https://doi.org/10.1016/j.ica.2020.119831>

This is a PDF file of an article that has undergone enhancements after acceptance, such as the addition of a cover page and metadata, and formatting for readability, but it is not yet the definitive version of record. This version will undergo additional copyediting, typesetting and review before it is published in its final form, but we are providing this version to give early visibility of the article. Please note that, during the production process, errors may be discovered which could affect the content, and all legal disclaimers that apply to the journal pertain.

© 2020 Elsevier B.V. All rights reserved.



## Crystal structure and infrared and Raman spectra of $K_3[Cr(CN)_5NO] \cdot 2H_2O$ , a member of an iconic family of complexes in coordination chemistry

Oscar E. Piro<sup>a</sup>, Gustavo A. Echeverría<sup>a,b</sup>, A. Navaza<sup>c</sup> and Jorge A. Güida<sup>b,d,e,\*</sup>

a LANADI e IFLP (CCT-La Plata), Departamento de Física, Facultad de Ciencias Exactas, Universidad Nacional de La Plata, CC67, 1900 La Plata, Argentina.

b Departamento de Ciencias Básicas Facultad de Ingeniería, Universidad Nacional de La Plata. 115 y 49. 1900 La Plata. Argentina.

c LPBC-CSSB, UMR CNRS 7033, Université Paris 13, 93017 Bobigny, France.

d CEQUINOR, Facultad de Ciencias Exactas, Universidad Nacional de La Plata, (CONICET-CCT La Plata), Boulevard 120 N° 1465, La Plata (1900), Argentina.

e Departamento de Básicas, Universidad Nacional de Luján, rutas 5 y 7, CC 6700, Luján, Argentina.

### Abstract

Potassium pentacyanonitrosylchromate(I) dihydrate salt,  $K_3[Cr(CN)_5NO] \cdot 2H_2O$ , forms spontaneously from aqueous solution below about 15 °C while the anhydrous salt is obtained above 20 °C. The molecular structure of the dihydrate has been determined by X-ray diffraction, taking full advantage of modern data collection, advanced space group and structure solution and refinement. It crystallizes in the monoclinic space group  $Cc$ , is isomorphic to the Mn(I) analog, and shows the pseudo-symmetry of space super-group  $C2/c$ . The  $[Cr(CN)_5NO]^{3-}$  ion has an umbrella-like conformation with the equatorial Cr-CN bonds slightly bent away from the Cr-NO link. The crystallographic study fills a gap left in the literature on accurate structural data for alkaline and alkaline-earth salts of  $[M(CN)_5NO]^{n-}$  ( $M = V, Cr, Mn, Fe$ ) series of coordination compounds. We also report here the solid-state vibration structure of the new compound, as probed by IR and Raman spectroscopy. Water mode assignments were assisted through deuterium enrichment. The thermal dehydration behavior complements structural and spectroscopic information on water molecules.

**Keywords:** single crystal X-ray diffraction; infrared and Raman spectroscopy; TGA and DTA thermal analysis; transition metal nitrosyls.

## 1. Introduction

Interest in transition metal nitrosyls, as a source of nitric oxide (NO), has been increased in the last two decades due to the discovery of the physiological properties of this molecule, which plays a fundamental role in the regulation of the cardiovascular system, in neuronal communication and in nonspecific defense against bacterial infection by macrophages, among other effects.[1] The nitroprusside anion  $[\text{Fe}(\text{CN})_5\text{NO}]^{2-}$ , related structurally to the chromium(I) analog, has continued to be used in the treatment of myocardium infarct.[2] Nitric oxide could also be released by hydrolysis of certain transition-metal nitrosyls or by irradiation with light of an adequate wavelength.[3] The possibility of NO release depends strongly on the nature of the M-N-O bonds. In this regard, structural crystallography complemented with spectroscopic methods provides an adequate methodology to study chemical bonds, with the aim to predict the possibility of NO release. [Potential pharmaceutical applications of the study compound will depend on a number of factors, including physicochemical, biological, and toxicity of ligands and metal.](#)

The systematic correlation of  $\nu(\text{NO})$ ,  $\nu(\text{MN})$  and  $\delta(\text{MNO})$  vibration mode frequency with bond distances and angles (M-N-O, M-C-N) for the first row transition metal series  $[\text{M}(\text{CN})_5\text{NO}]^{n-}$  from V to Fe could be useful to understand the nature of bonds, to compare the  $\pi$ -backbonding with NO and CN acceptor groups and then to predict the chemical behavior expected for these anions with different reactivities.

The family of transition metal nitrosyls  $[\text{ML}_5\text{NO}]^{2-}$  (M=Fe, Ru, Os; L=CN, NO<sub>2</sub>, OH, Cl) presents additional interest because some of them exhibit one or two very long-lived excited metastable states (NO linkage isomers) when they are irradiated at low temperature with light of wavelength lying in the visible or near-UV region. The color change exhibited upon generation of the new states has been proposed as the basis of an information storage system, since information can be written/read and erased reversibly using light of two different wavelengths.[4] All our attempts to generate metastable states in  $\text{K}_3[\text{Cr}(\text{CN})_5\text{NO}]$  at 77 K, similar to those reported for the  $[\text{M}(\text{CN})_5\text{NO}]^{n-}$  (M=Mn, Fe) [4, 5] series were not successful.

Furthermore,  $[\text{Cr}(\text{CN})_5\text{NO}]^{3-}$  anion is of intrinsic interest because it is an example of a stable complex involving an unusual metal oxidation state (Cr(I), considering nitrosyl as  $\text{NO}^+$  or  $\{\text{CrNO}\}^5$  according to Enemark-Feltham notation [6]).

### 1.1 Historic background

$[\text{Cr}(\text{CN})_5\text{NO}]^{3-}$  complex is a member of an iconic family in coordination chemistry, namely the pentacyanonitrosylmetallates,  $[\text{M}(\text{CN})_5\text{NO}]^n$ ; M: V, Cr, Mn, Fe. However, the growth of good quality single crystals of alkaline and alkaline-earth salts of the chromium complex, adequate for precise structural X-ray diffraction, proved elusive. In fact, employing single-crystal X-ray diffraction data collected on rotation photographs, Vannenberg reported in 1966 the crystal structure of  $\text{K}_3[\text{Cr}(\text{CN})_5\text{NO}]$  in the orthorhombic space group  $Pcn2$ . [7] The electron density maps showed the chromium ion surrounded by six ligands in an impossible regular octahedral arrangement. This was attributed to a high degree of disorder of the complex that prevented to distinguish between the nitrosyl and the cyanide ligands and therefore to obtain precise intramolecular bond distances and angles. [7]

Enemark *et al.* [8] crystallized an ordered  $[\text{Cr}(\text{CN})_5\text{NO}]^{3-}$  complex using the bulky counter-ion trisethylenediammincobalt(III) in the  $[\text{Co}(\text{C}_2\text{H}_8\text{N}_2)_3][\text{Cr}(\text{CN})_5\text{NO}]\cdot 2\text{H}_2\text{O}$  salt. They determined the monoclinic space group  $P2_1/c$  from systematic absences observed in the X-ray diffraction pattern of preliminary precession and Weissenberg photographs and then solved the structure by Patterson and Fourier methods from data collected on a Supper-Pace automated diffractometer, employing Weissenberg geometry and a scintillation detector. However, it was necessary to resort to a third data set collected on a Picker automatic diffractometer to achieve a successful refinement. The crystallographic agreement factor was  $R1 = 0.053$  and Cr-ligand bond distance errors were in the 0.011-0.014 Å range, while C-N and N-O bond lengths were determined with errors from 0.012 to 0.013 Å. The authors could not locate the H-atoms in their difference Fourier map phased on the heavier atoms. [8]

Prompted by the successful crystallization of an hydrated potassium salt of  $[\text{Cr}(\text{CN})_5\text{NO}]^{3-}$  at carefully controlled temperature and the availability of modern X-ray diffraction data collection and advanced space group and crystal structure determination and refinement, including the handling of twinning, we undertook the crystal structure determination of the salt with the aim, in part, to provide more precise bond distances and angles for the complex.

In this work, the infrared and Raman spectra of  $K_3[Cr(CN)_5NO].2H_2O$  are also reported, including studies on deuterium-enriched samples. Thermal decomposition of the compound up to 200 °C was also studied by TGA-DTA under a nitrogen atmosphere.

## 2. Experimental

### 2.1. *Synthesis and crystallization*

The title compound was prepared following a method reported in the literature.<sup>[9]</sup> Depending on the temperature of the saturated aqueous solution, two crystalline forms of the complex (easily recognized by its crystal habit) were found by the evaporation of the solvent. Below 15°C crystals of  $K_3[Cr(CN)_5NO].2H_2O$  were grown as an elongated prism, while the anhydrous form crystallized as rhombic platelets above 20°C. Crystals of  $K_3[Cr(CN)_5NO].2H_2O$ , adequate for structural X-ray diffraction and spectroscopic measurements, were grown at about 4 °C in a refrigerator.

Partially deuterated samples were prepared by dissolving anhydrous  $K_3[Cr(CN)_5NO]$  in the minimum volume of  $D_2O$  below 10 °C. The solid crystallized from the saturated solution by the  $D_2O$  evaporation on a rotary evaporator at a constant temperature.

### 2.2. *Sample preparation for the spectroscopic measurements*

For the recording of the infrared spectra, the anhydrous salt was prepared following a general procedure and then dispersed in KBr granules. For the Raman spectra, the laser beam was focused on the finely divided powdered sample. Sample preparation of the dihydrate salt to be submitted both to infrared and Raman spectroscopy was carried out in a cold room (below 10°C) by grinding the crystals in Nujol or Halocarbon to avoid dehydration during the measurement.

Of all the commercially available oils suitable for vibration spectroscopy, Nujol was chosen because it presents broad transparent windows. In fact, its absorption spectral regions cover 3000-2800, 1500-1300 and 750-700  $cm^{-1}$  range and only overlaps the water  $\delta(HOD)$  bands at around 1400  $cm^{-1}$ . No other overlapping region was registered for neither the bands of the complex nor the ones of isotopically pure or partially deuterated crystallization water molecules.

For measurements around  $1400\text{ cm}^{-1}$  the samples were prepared as described above but now in Halocarbon oil, whose absorption bands appear below  $1350\text{ cm}^{-1}$ . For infrared measurements, the mull was spread between CsI windows. To avoid damaging the samples by heating during the scanning, the sample-containing window was carried close to the spectrometer inside a desiccator which was kept below  $10^\circ\text{C}$ . Then the CsI windows were quickly placed in the spectrometer compartment. The samples prepared in this way showed no damage for at least 10 minutes after the end of the scanning.

To avoid heating the sample by the laser beam during the Raman experiments, a continuous stream of cooled nitrogen was passed through the sample holder such as to keep the temperature below  $15^\circ\text{C}$ .

### 2.3. X-ray diffraction data

The measurements were performed on an Oxford Xcalibur, Eos, Gemini CCD diffractometer employing graphite-monochromated  $\text{MoK}\alpha$  ( $\lambda = 0.71073\text{ \AA}$ ) radiation. To avoid dehydration, the single crystal sample was mounted embedded in an oil drop. X-ray diffraction intensities were collected ( $\omega$  scans with  $\vartheta$  and  $\kappa$ -offsets), integrated and scaled with CrysAlisPro [10] suite of programs. The unit cell parameters were obtained by least-squares refinement (based on the angular settings for all collected reflections with intensities larger than seven times the standard deviation of measurement errors) using CrysAlisPro.

The structure was solved with the procedure described by convenience in Section 3.1 and implemented in SHELXT [11] and the corresponding non-H molecular model refined with anisotropic displacement parameters employing SHELXL.[12] At this stage, it turned out that the absolute structure could not be determined with certainty as the Flack parameter was equal to  $0.24(3)$ . This parameter is the fractional contribution to the diffraction pattern due to the molecule racemic twin and for the correct enantiomeric crystal, it should be zero to within experimental accuracy.[13] Therefore, the structure was further refined as a racemic twin, giving an occupancy of  $0.26(3)$  for the minor enantiomeric contributor.

The water H-atoms were located in a difference Fourier map and refined at their found positions with isotropic displacement parameters and O-H and H...H distances restrained to target values

of 0.86(1) and 1.36(1) Å. Crystal data, data collection procedure, and refinement results are summarized in Table 1.

CCDC 1970978 (for  $K_3[Cr(CN)_5NO].2H_2O$ ) contains the supplementary crystallographic data for this paper. These data can be obtained free of charge from The Cambridge Crystallographic Data Centre.

#### 2.4. *Solid state infrared absorption and Raman dispersion spectra*

The infrared spectra were recorded on a Bruker 113v equipped with a mid-IR DTGS detector working at a resolution of 4  $cm^{-1}$  in the 4000–250  $cm^{-1}$  region. A satisfactory signal-to-noise ratio was obtained with 200 scans.

The Raman spectra covering the region between 3500 and 100  $cm^{-1}$  were obtained with a FRA 106 accessory mounted on a Bruker IFS 66 FTIR instrument (500 scans and 4  $cm^{-1}$  resolution), using the 1064 nm excitation line from a Nd–YAG laser working at a power of 150 mW.

#### 2.5. *TGA and DTA thermal analysis*

TGA-DTA measurements of  $K_3[Cr(CN)_5NO].2H_2O$  were performed with a Shimadzu TGA-50 and DTA-50H units in the 15–200 °C range, at a heating rate of 10 °C/min and with a nitrogen flow of 50 ml/min. The DTA unit was calibrated using potassium nitrate and indium and the TGA with calcium oxalate monohydrate.

### 3. Results and discussion

#### 3.1. *Crystal structure*

Recent developments of crystal space group and structure determination from X-ray diffraction do not rely exclusively on sometimes ambiguous extinctions and intensity statistics. In this context, it has been observed that frequently crystal structures can be solved more easily in the underlying triclinic space group  $P1$  [14] and also that the correct space group can be determined from  $P1$  structure factor phases, [15,16] rather than from atomic positions. In a particular application of these observations, Sheldrick implemented an integrated space-group and crystal-structure determination procedure [11] that combines Patterson with density modification and dual-space recycling methods. The algorithm only requires as input

information the Laue group and the identity of the atoms expected in the solid and can be succinctly described as follows:

i) From the X-ray diffraction data extended to  $P1$ , the structure is solved in this space group by Patterson superposition and dual-space recycling methods to obtain optimal  $P1$  phases.

ii) The correct space group is then determined from the  $P1$  phases as follows: Let us consider a candidate space group  $G$  of symmetry elements  $(\mathbf{P}_m, \mathbf{t}_m)$ , where  $\mathbf{P}_m$  is the point group operation,  $\mathbf{t}_m$  the associated translation vector, and the suffix  $m$  runs over the space group symmetry elements. The ‘star’ of the reciprocal vector  $\mathbf{h}$  is defined by the symmetry operation:  $\mathbf{h}_m = \mathbf{h}\mathbf{P}_m$ . If  $\Delta\mathbf{r}$  is the displacement vector that refers to the  $P1$  structure to the proper unit cell origin of the space group  $G$ , then the  $P1$  phases  $\phi(\mathbf{h})$  and  $\phi(\mathbf{h}_m)$  change to  $\phi'(\mathbf{h}) = \phi(\mathbf{h}) + 2\pi\mathbf{h} \cdot \Delta\mathbf{r}$  and  $\phi'(\mathbf{h}_m) = \phi(\mathbf{h}_m) + 2\pi\mathbf{h}_m \cdot \Delta\mathbf{r}$ . As in the space group  $G$  these phases are symmetry-related through  $\phi'(\mathbf{h}) - \phi'(\mathbf{h}_m) = 2\pi\mathbf{h} \cdot \mathbf{t}_m$ , there results that for the correct space group and origin shift,

$$q = \phi(\mathbf{h}_m) - \phi(\mathbf{h}) + 2\pi[\mathbf{h} \cdot \mathbf{t}_m + (\mathbf{h}_m - \mathbf{h}) \cdot \Delta\mathbf{r}] \quad (1)$$

should be close to zero (module  $2\pi$ ). A measure of the departure from the ideal value of zero is provided by a phase error ( $\alpha$ ) which varies from 0 to 1 (for random phases). The  $P1$  phases are employed in Equation (1) to find the candidate space groups  $G$  (compatible with the known Laue group) and the corresponding cell origin shifts  $\Delta\mathbf{r}$ .

iii) The phases are then symmetry-averaged in the candidate space groups and then used to calculate improved electron density maps.

iv) A chemical formula is proposed for the solid-state compound based on the integrated electron density around the peaks of the maps and its assignment to the assumed atomic species in the crystal.

v) The selection of the correct space group and structure solution among the trials is made on the basis of diverse figures of merit, including the  $R1$ -factor,  $R_{\text{weak}} (= \langle E_{\text{calc}}^2 \rangle)$  over the 10% of unique reflections with the smallest  $E_{\text{obs}}$  and the phase error ( $\alpha$ ), which should all be the smallest for the right solution.

The result of the above procedure applied to the X-ray diffraction data of  $\text{K}_3[\text{Cr}(\text{CN})_5\text{NO}]\cdot 2\text{H}_2\text{O}$  crystal assuming the Laue group  $C2/m$  ( $C_{2h}$ ) and the presence in the solid of Cr, K, O, N and C



atomic species is shown in Table 2. From this table it can be appreciated that the procedure clearly selects the non centre-symmetric space group  $Cc$  as having the best indicators. It can also be noted that the program misassigned as carbon one N-atom and as oxygen three N-atoms, a minor problem that probably arises in part due to the closeness of their number of atomic electrons.

An ORTEP [17] plot of  $[\text{Cr}(\text{CN})_5\text{NO}]^{3-}$  ion is shown in Fig. 1 and corresponding bond distances and angles within the complex are in Table 3 and short contacts around the potassium ions are in Table 4. The chromium(I) complex is isomorphic to the manganese(I) analog, namely  $\text{K}_3[\text{Mn}(\text{CN})_5\text{NO}]\cdot 2\text{H}_2\text{O}$ , reported more than fifty years ago by Tullberg and Vannenberg [18, 19] employing X-ray diffraction data collected photographically with the Weissenberg method. From the observed extinctions, the authors determined  $C2/c$  and  $Cc$  as the possible space groups. Assuming first the centre-symmetric space group  $C2/c$ , they determined from a Patterson map that the manganese atom was located at a crystallographic inversion centre. Ruling out this possibility for  $[\text{Mn}(\text{CN})_5\text{NO}]^{3-}$ -complex, they finally adopted the space group  $Cc$  as the correct one. [18, 19]

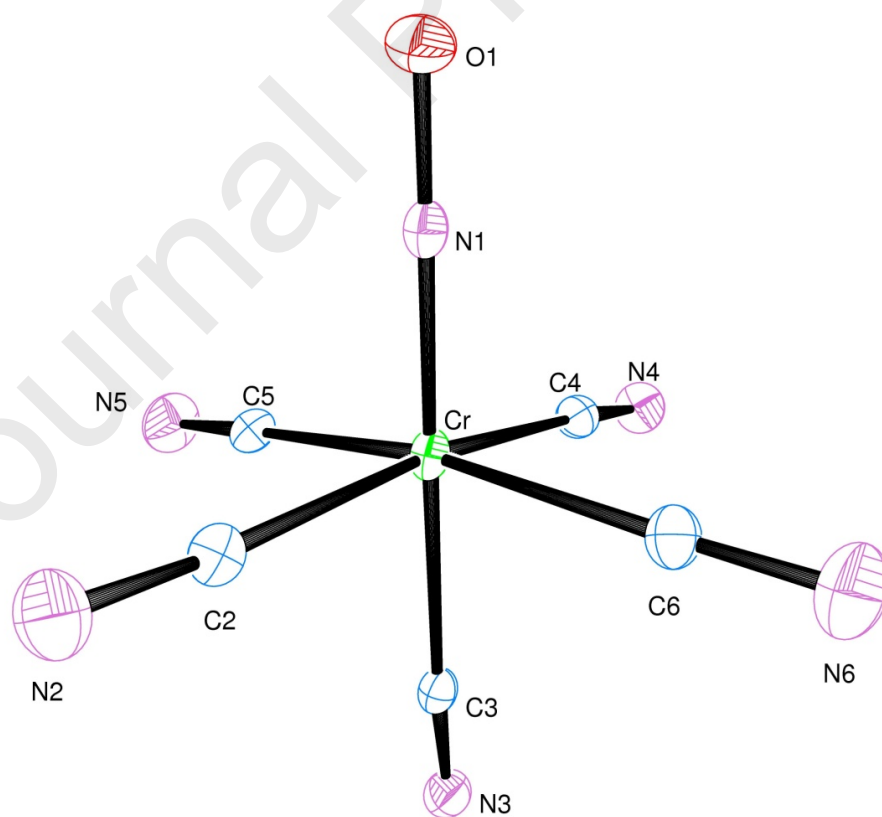


**Fig. 1.** Drawing of potassium pentacyanonitrosylchromate(I) complex in  $K_3[Cr(CN)_5NO].2H_2O$  salt showing the labeling of the atoms and their displacement ellipsoids at the 30 % probability level

The chromium(I) complex shows equatorial Cr-CN bond distances from 2.062(4) to 2.072(4) Å [average(dispersion) = 2.067(4) Å] and a significantly longer axial Cr-CN length of 2.100(4) Å. Cr-NO length is 1.699(3) Å and nitrosyl N-O bond length is equal to 1.209(4) Å. Cyanide C-N bond lengths are in the 1.145(7)-1.151(6) Å range [average(dispersion) = 1.148(2) Å].

The complex exhibits an approximate  $C_{4v}$  symmetry and has an umbrella-like conformation with the ligands projected outwardly from the metal centre. The equatorial Cr-CN bonds are slightly bent away from the Cr-NO link. In fact ON-Cr-C(eq)N bond angles are larger than  $90^\circ$  [from 90.1(2) to 98.2(2) $^\circ$ ] and equatorial *trans* NC-Cr-CN angles are significantly less than  $180^\circ$  [171.6(2) and 170.8(2) $^\circ$ ], contrasting with the near straight angle of axial ON-Cr-C(ax)N bond [equal to 177.8(2) $^\circ$ ]. Cr-C-N angles are also close to straight ones [from 173.5(4) to 178.1(5) $^\circ$ ] and  $\angle(\text{Cr-N-O}) = 174.3(3)^\circ$ . Our structural results for the complex are in general agreement with early data for  $[Co(C_2H_8N_2)_3][Cr(CN)_5NO].2H_2O$  [8] and also with more recent determinations of  $[Cr(CN)_5NO]^{3-}$  salts involving even bulkier counter-ions. [20, 21]

Potassium ion K1 is in a distorted four-fold coordination with three cyanide N-atoms [K...N short contact distances from 2.801(4) to 2.999(5) Å] and one nitrosyl oxygen atom [d(K...O) = 2.829(4) Å]. Potassium ions K2 and K3 are in a very similar distorted nine-fold polyhedral coordination with three water oxygen atoms [K...Ow contact distances from 2.803(4) to 3.263(4) Å], five cyanide N-atoms [K...N distances in the range from 2.850(5) to 3.321(6) Å] and one nitrosyl oxygen [K...O distances of 3.021(3) Å (K2) and 3.185(3) Å (K3)]. This is not accidental as it turns out that the  $Cc$  crystal presents the higher pseudo-symmetry of space supergroup  $C2/c$ , which renders centre-symmetric the complex, inversion-related to each other the potassium K(2) and K(3) ions and the two water O1w and O2w oxygen atoms, and locate on a two-fold axis the potassium K(1) ion. The origin of the broken symmetry is mainly due to the slight differences between the Cr-NO and N-O bond distances and the corresponding metrics of cyanide ligand in the distorted octahedral  $[Cr(CN)_5NO]$  complex. The correctness of space group  $Cc$  is further sustained by the slight asymmetry between the water molecules observed in the IR

spectra of normal and deuterium-enriched samples (see Sect. 3.2.1) and also in the DTA data (Sect. 3.3).

As shown in Figure 2, the  $\text{K}_3[\text{Cr}(\text{CN})_5\text{NO}]\cdot 2\text{H}_2\text{O}$  monoclinic solid can be described as a layered structure parallel to the crystal (100) plane. It consists of slabs of  $[\text{Cr}(\text{CN})_5\text{NO}]^{3-}$  anions and potassium K1 cations intercalated with sheets of K2 and K3 ions in a distorted honeycomb arrangement filled with the water molecules. Interestingly, the orthorhombic anhydrous salt [6] shows a similar layered structure where the sheets of potassium ions, now deprived of water, exhibit a distorted hexagonal arrangement. In fact, there is a close structural relationship between the crystals. Figure 1 includes a view of a slightly distorted orthorhombic unit cell of the anhydrous compound embedded in the monoclinic lattice. The transformation between unit cell vectors of the orthorhombic (*o*) and monoclinic (*m*) lattices is  $\vec{a}_o = \vec{a}_m + \vec{c}_m/2$ ;  $\vec{b}_o = \vec{b}_m + \vec{c}_m/2$  and  $\vec{c}_o = -\vec{b}_m + \vec{c}_m/2$ .

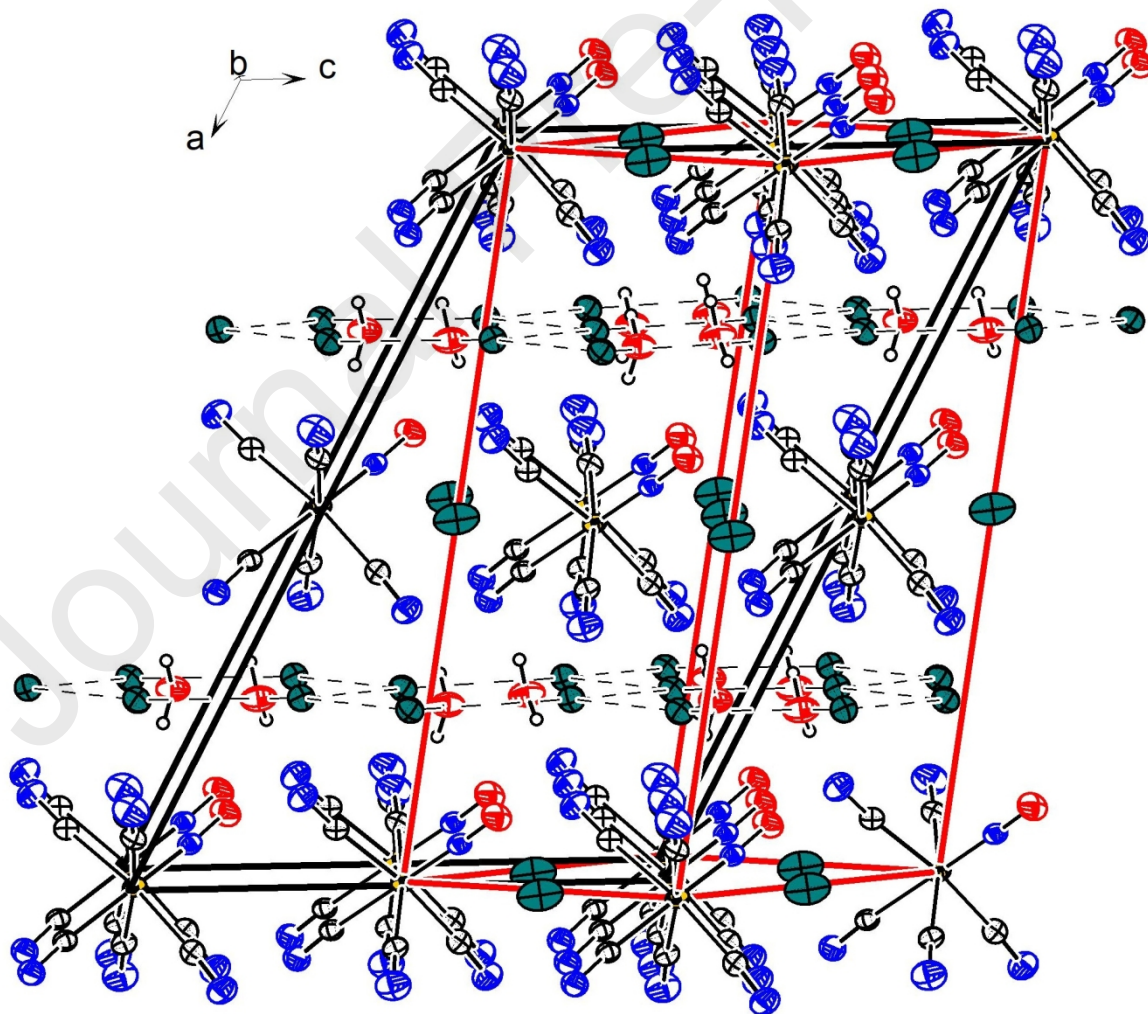


**Fig. 2.** Crystal packing view down **b** of monoclinic  $K_3[Cr(CN)_5NO].2H_2O$  salt, showing the  $[Cr(CN)_5NO]^{3-}$  and potassium (K1) layers and those formed by potassium K2 and K3 cations and the water molecules. The dashed lines joining neighboring potassium in these latter layers are a guide to the eyes. For clarity, H-bonds are not shown. In red line are drawn the distorted orthorhombic unit cell of the anhydrous salt embedded in the monoclinic lattice of the dihydrate.

The lattice is further stabilized by two medium strength and linear Ow-H...N bonds involving both water molecules and cyanide N-atoms as acceptors [H...N distances both equal of 2.01(2) Å and Ow-H...N angles of 169(4) and 172(5)°]. These and other much weaker and bent H-bonds are detailed in Table 5.

### 3.2. Infrared and Raman spectra

Early infrared absorption spectra of the chromium(I) complex in its potassium salt, assumed as a monohydrate, were first reported by Griffith and co-workers. [9, 22] As part of an IR study on a series of transition metal complexes, Miki (1968) reported the frequency of  $\nu(NO)$  stretching mode of normal and  $^{15}N$  isotopically-enriched nitrosyl in  $K_3[Cr(CN)_5NO].H_2O$  salt. [23]

We shall present here the vibration structure of  $K_3[Cr(CN)_5NO].2H_2O$  as probed by infrared absorption and Raman dispersion spectroscopy and compare it with the anhydrous analog, for which the Raman spectrum has not yet been reported.

#### 3.2.1 Water vibrations

Since, as expected, the water bands went undetected in the Raman spectra, the attention was focused on the infrared absorption. To differentiate the water bands that could be overlapped with some vibration modes of  $[Cr(CN)_5NO]^{3-}$ -complex ion, the samples were partially enriched with deuterium (D). The comparison of the infrared spectra of  $K_3[Cr(CN)_5NO].2H_2O$  with that of the anhydrous analog and the spectral shifts observed in the deuterated samples, allowed us to perform a reliable identification of bands and mode assignments. Fig. 3 shows the infrared spectra of  $K_3[Cr(CN)_5NO].2H_2O$  with different (D/H)ratio, measured at about 10°C in the absorption region of  $H_2O$ , HDO, and  $D_2O$  vibration modes.

The spectrum A corresponds to the natural sample of the dihydrate, the spectrum B to the partially deuterated sample (60% D enriched) muller in halocarbon, the spectrum C to a partially enriched sample (40% D) in Nujol mull and the spectrum E to the most deuterium-enriched

sample (70% D) in Nujol mull. It can be appreciated that, as expected, the intensity of deuterated bands grows with deuterium content hence helping band identification.

The bands at 3592 and 3392  $\text{cm}^{-1}$  can easily be assigned to the water  $\nu(\text{OH})$  antisymmetric ( $\nu_3$ ) and symmetric ( $\nu_1$ ) stretching modes, respectively. Due to the partial enrichment with deuterium, the corresponding OD stretching modes are shifted to 2657 and 2502  $\text{cm}^{-1}$ , respectively.[24]

Water bending  $\delta(\text{H}_2\text{O})$  modes are commonly observed in the 1600-1700  $\text{cm}^{-1}$  region as sharp bands of medium intensity.[24] In this region, the infrared spectra of  $\text{K}_3[\text{Cr}(\text{CN})_5\text{NO}]\cdot 2\text{H}_2\text{O}$  show a wide and strong band composed of three features at 1658, 1646 and 1630  $\text{cm}^{-1}$ . Then, the water bending should be overlapped with the very strong (low frequency)  $\nu(\text{NO})$  mode. Upon enrichment with deuterium, bands at 1646 and 1630  $\text{cm}^{-1}$  decrease their intensity (see Fig. 3) and therefore these bands are assigned to  $\delta(\text{H}_2\text{O})$  ( $\nu_2$ ) bending mode. Consequently, the remaining band at 1658  $\text{cm}^{-1}$  should correspond to the  $\nu(\text{NO})$  stretching mode (see Sect. 3.2.2). The corresponding  $\delta(\text{HOD})$  bending vibrations usually appear at about 1420  $\text{cm}^{-1}$ . [24] These bands are only seen when the samples are dispersed in the halocarbon mull because Nujol oil shows strong absorption in the 1500-1300 $\text{cm}^{-1}$  region. The weak bands observed in halocarbon at 1465, 1425 and 1411  $\text{cm}^{-1}$  are then assigned to  $\delta(\text{HOD})$  mode (see spectrum B in Fig. 3). The  $\text{D}_2\text{O}$  bending bands are expected to be shift to even lower frequencies, at about 1200  $\text{cm}^{-1}$  [24]. The bands at 1208 and 1197  $\text{cm}^{-1}$ , whose intensity increases with the deuterium content, are thus assigned to this vibration mode.[24, 25]

The very weak band at 2396  $\text{cm}^{-1}$ , whose intensity increased with the D-enrichment, is assigned to the first  $\delta(\text{D}_2\text{O})$  overtone [ $2\delta(\text{D}_2\text{O})$ ].

Bands assignments for the water bands and partially deuterated samples proposed in Table 6 compare favorably with those reported for similar systems:  $\text{K}_3[\text{Mn}(\text{CN})_5\text{NO}]\cdot 2\text{H}_2\text{O}$  (same stoichiometry and crystal structure) [26] and  $\text{Na}_2[\text{Fe}(\text{CN})_5\text{NO}]\cdot 2\text{H}_2\text{O}$ . [27]

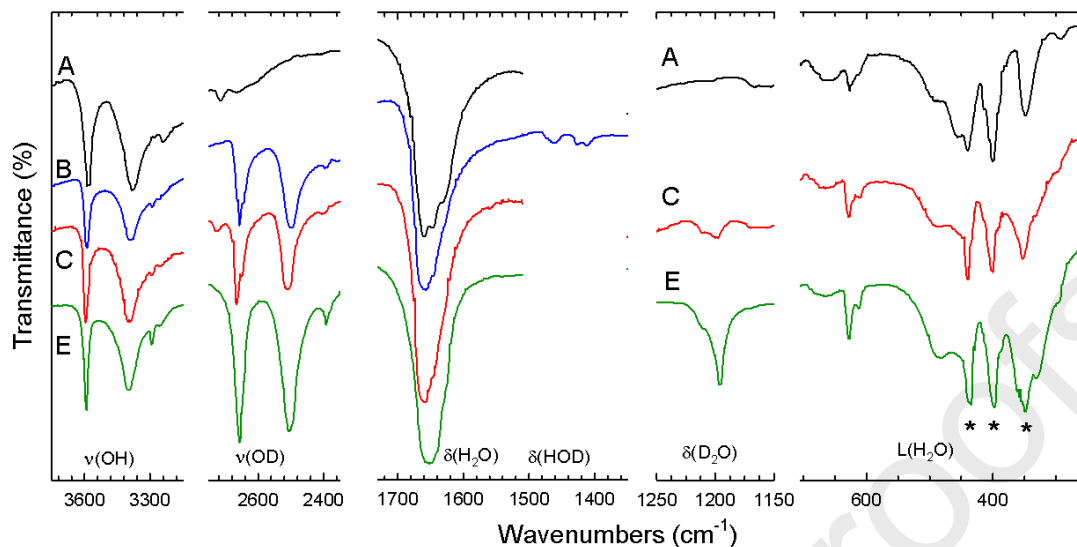


**Fig. 3.** Infrared spectra of  $\text{K}_3[\text{Cr}(\text{CN})_5\text{NO}]\cdot 2\text{H}_2\text{O}$  in the water vibration regions with different deuterium (D) content. A) Normal sample in Nujol mull, B) 60% D-enriched in halocarbon mull (the region below  $1250\text{ cm}^{-1}$  were suppressed to avoid confusion with the oil bands); C) 40% D-enriched in Nujol mull E) 70% D-enriched in Nujol mull. All Nujol mull spectra in the  $1510\text{--}1350\text{ cm}^{-1}$  region were suppressed to avoid confusion with the oil bands. \*Denotes  $\nu(\text{Cr-C})$  or  $\delta(\text{CrCN})$  vibrations.

Bands due to water librations are observed below  $750\text{ cm}^{-1}$ . Some of them are overlapped with modes of the anion, namely  $\nu(\text{Cr-N})$ ,  $\delta(\text{CrNO})$ ,  $\nu(\text{Cr-C})$  and  $\delta(\text{CrCN})$ . Since the complex in the anhydrous sample only shows five sharp and well-defined bands in this region, the librations of water in the dihydrate were recognized through spectra comparison. Additional evidence of water libration modes in the spectra was found with the deuterium-enriched samples. In fact, libration bands undergo intensity reduction and slight shifts towards high or low frequencies upon deuterium exchange. All these effects were considered in the assignment of water bands gathered in Table 6.

**3.2.2 Vibrational modes of the complex:** The infrared and Raman spectra of  $\text{K}_3[\text{Cr}(\text{CN})_5\text{NO}]$  and  $\text{K}_3[\text{Cr}(\text{CN})_5\text{NO}]\cdot 2\text{H}_2\text{O}$  are compared in Fig. 4. Bands details are shown in the expanded spectra of Fig. 5. Bands assignments are in Table 7.



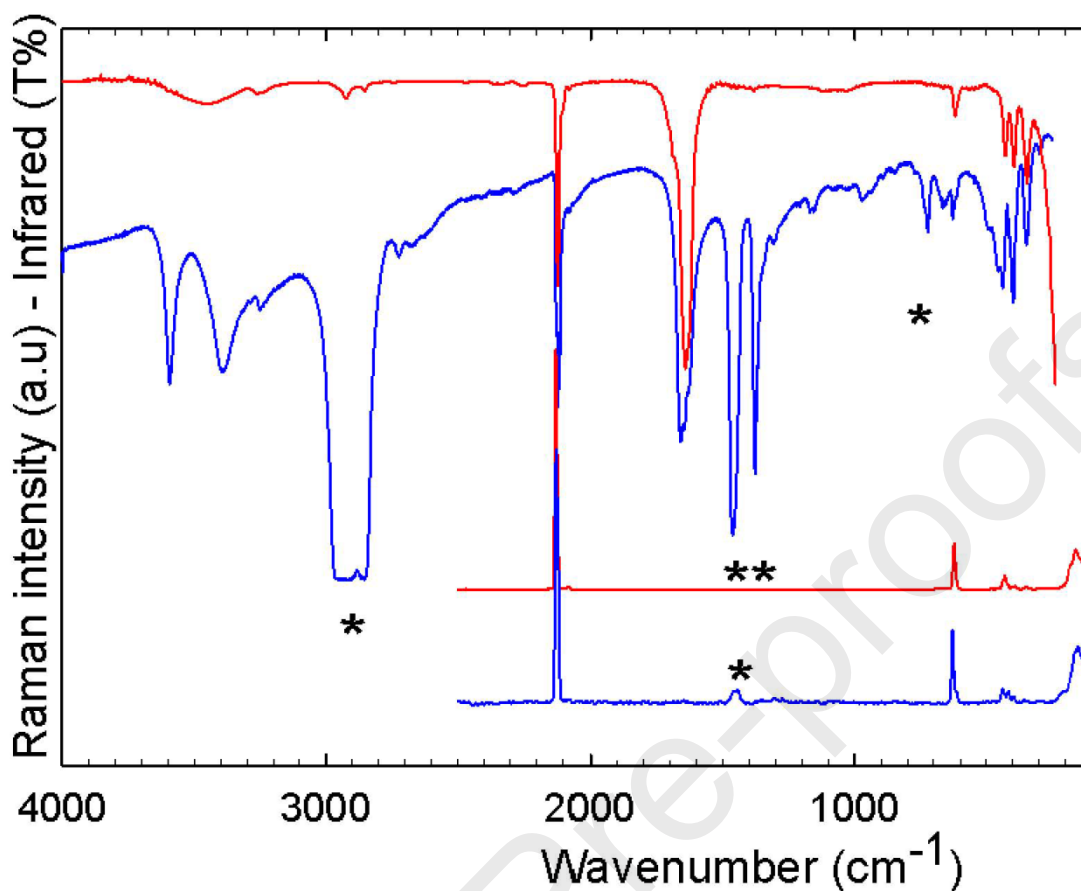


**Fig. 4.** Infrared and Raman spectra of  $K_3[Cr(CN)_5NO]$  (red) and  $K_3[Cr(CN)_5NO].2H_2O$  (blue) below 15 °C. \* denotes Nujol bands.

**3.2.3 CN stretching modes:** The CN stretching modes can easily be identified in the 2200-2000  $cm^{-1}$  region of both the infrared and Raman spectra since they give rise to sharp and medium-intensity bands. [28] Their relative positions in the spectra are the result of electron flow between the cyanide groups and the metal; in fact, CN acts as  $\sigma$ -donator and  $\pi$ -acceptor.  $\sigma$ -donation to the metal rises the CN stretching frequency while the acceptance of electrons via  $\pi$ -interaction decreases it ( $\pi$  back-bonding). Since Cr(I) ion is electron-rich the CN frequency is expected to be rather low in  $[Cr(CN)_5NO]^{3-}$ . For the above reasons, the main band at 2125  $cm^{-1}$  and a shoulder at 2119  $cm^{-1}$  are assigned to the CN bands in the anhydrous complex and the bands at 2125, 2117 and 2112  $cm^{-1}$  to the dihydrate. The CN stretching mode in nitroprusside ion ( $[Fe(II)(CN)_5NO]^{2-}$ ), for comparison, is observed at higher frequencies (in the 2180-2130  $cm^{-1}$  range), because the larger oxidation state of the iron(II) reduces the electron back-bonding flow to the CN ligands, in contrast to the behavior observed for the chromium(I) analog. The CN stretching band, which is

observed in the infrared spectra almost as a single band in the anhydrous compound, splits into three components in the dihydrate, probably due to the interactions of CN groups with K and water molecules detailed in the crystal structure section.

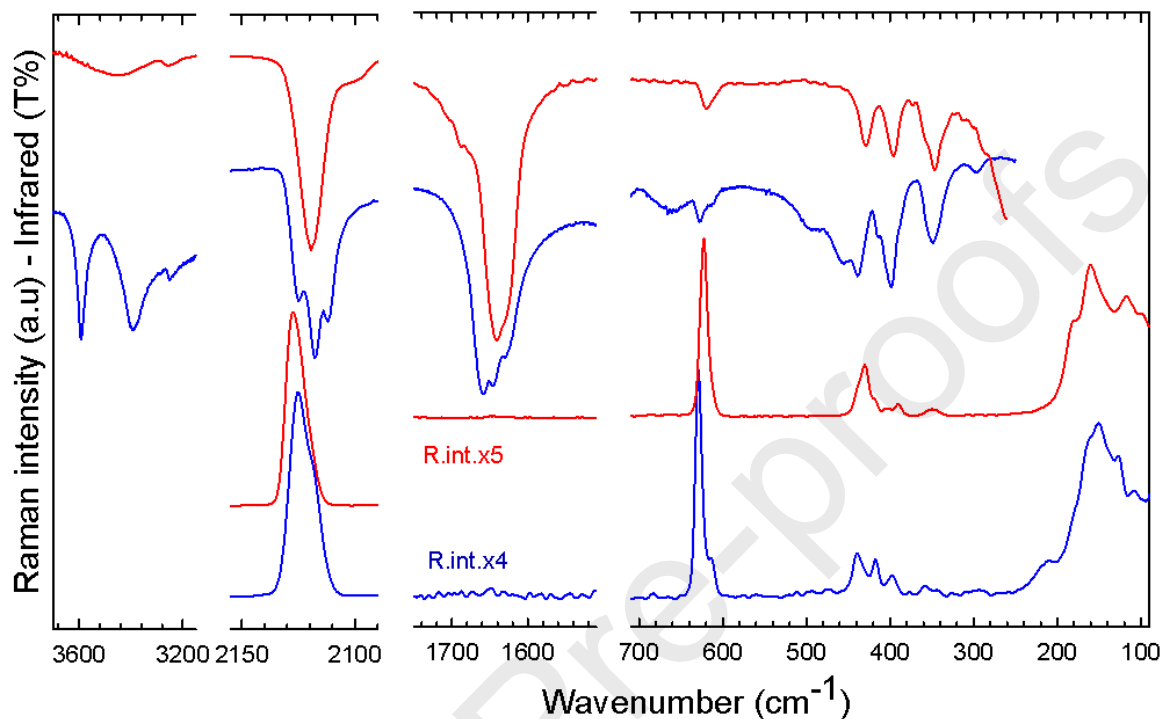


**Fig. 5.** Infrared and Raman spectra of  $\text{K}_3[\text{Cr}(\text{CN})_5\text{NO}]$  (red) and  $\text{K}_3[\text{Cr}(\text{CN})_5\text{NO}]\cdot 2\text{H}_2\text{O}$  (blue) (measured below 15 °C). For convenience, the intensity of Raman spectra below 1700  $\text{cm}^{-1}$  was multiplied by 4 and 5 for the dihydrate and anhydrous complexes, respectively. For clarity, Nujol bands were suppressed.

**3.2.4 NO stretching mode:** The NO stretching mode gives rise in the 2000-1500  $\text{cm}^{-1}$  spectral region to very strong and wide absorption bands in the infrared and very weak dispersion in Raman,<sup>[28]</sup> a behavior that helps its identification. The infrared bands at 1658 and 1643  $\text{cm}^{-1}$  are respectively assigned to the  $\nu(\text{NO})$  mode of the dihydrate and anhydrous. This mode could not be detected in the Raman spectrum of either compound. NO mode was observed at a quite low frequency as a consequence of the  $\pi$ -backbonding. Nitrosyl ligand is more sensitive than cyanide groups with regard to this backbonding effect. For comparison,  $\nu(\text{NO})$  mode is observed at 1945  $\text{cm}^{-1}$  in nitroprusside ion (sodium salt) and at 2008  $\text{cm}^{-1}$  in  $\text{K}[\text{IrCl}_5\text{NO}]$  at 77 K.<sup>[29]</sup>

To illustrate this phenomenon, Fig. 6 compares the  $\nu(\text{NO})$  and  $\nu(\text{CN})$  stretching frequencies reported for the series of related anions:  $[\text{M}(\text{CN})_5\text{NO}]^{3-}$  where  $\text{M} = \text{V}, \text{Cr}, \text{Mn}$  (at a formal oxidation state I). The  $\nu(\text{CN})$  frequencies remain constant but the  $\nu(\text{NO})$  considerably increases with the atomic number of transition metal. In this figure, it is also included the nitroprusside ion for which is reported one of the highest  $\nu(\text{NO})$  frequency (1945  $\text{cm}^{-1}$ , sodium salt) of all transition metal nitrosyls.<sup>[30]</sup>



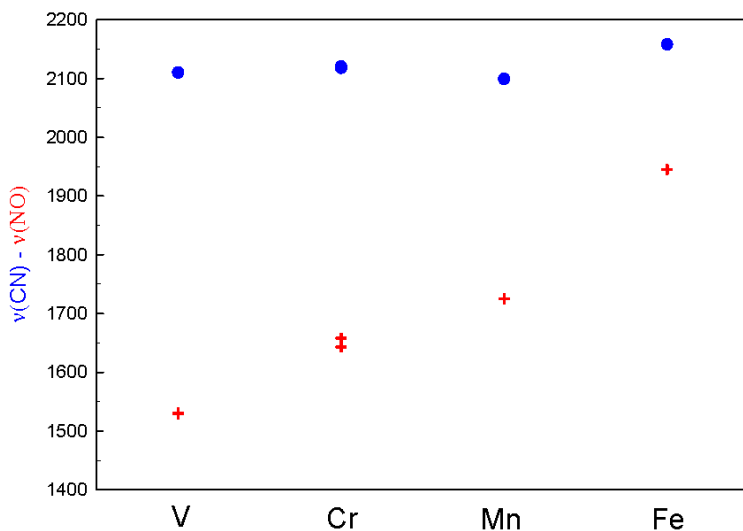


**Fig. 6.** Plot of  $\nu(\text{NO})$  (+) and  $\nu(\text{CN})$  (•) for the series of related ions:  $[\text{M}^{\text{I}}(\text{CN})_5\text{NO}]^{3-}$ . The values for  $[\text{Fe}^{\text{II}}(\text{CN})_5\text{NO}]^{2-}$  ion (in the sodium salt) is also included for comparison.

**3.2.5. Low-frequency spectral region:** The anion skeletal modes along with the water libration and lattice modes appear in the  $700\text{-}100\text{ cm}^{-1}$  region. The CrNO vibrations are observed in the  $600\text{-}650\text{ cm}^{-1}$  range for  $[\text{M}(\text{CN})_5\text{NO}]$  (M: Cr, Mn, Fe) systems. The  $\delta(\text{CrNO})$  bending and  $\nu(\text{CrN})$  stretching band assignments are proposed by comparison with other  $[\text{M}(\text{CN})_5\text{NO}]$  (M: Mn, Fe) similar systems and with spectroscopic studies in  $^{15}\text{N}$ -enriched series of complexes  $[\text{CrL}_5\text{NO}]^{\pm n}$  with  $\text{L}=\text{CN}, \text{NH}_3$ .<sup>[23]</sup> The  $\delta(\text{CrCN})$  and  $\nu(\text{CrC})$  modes are observed at frequencies below  $550\text{ cm}^{-1}$ . Water libration bands that appeared in this region of the infrared spectra were identified by enrichment with deuterium (see Sect. 3.2.2) and by comparison with the spectra of the anhydrous analog (see Sect. 3.2.1). The CrC stretches and CrCN deformations are tentatively assigned by comparison with other similar systems and with assignments reported for the nitroprusside ion.<sup>[31]</sup>

### 3.3 Thermal measurements

The first stage of  $\text{K}_3[\text{Cr}(\text{CN})_5\text{NO}]\cdot 2\text{H}_2\text{O}$  thermal decomposition proceeds in the  $25\text{-}70\text{ }^\circ\text{C}$  range (see Fig. 7), at lower temperatures than in other related complexes like  $\text{Na}_2[\text{Fe}(\text{CN})_5\text{NO}]\cdot 2\text{H}_2\text{O}$ <sup>[32]</sup> and  $\text{Ba}_3[\text{Cr}(\text{CN})_5\text{NO}]_2\cdot 8\text{H}_2\text{O}$ .<sup>[33]</sup> The DT curve shows two endothermic peaks (similar intensities) centered at  $42$  and  $60\text{ }^\circ\text{C}$ . A total mass loss of  $7.7\%$  is registered in the corresponding TG curve, which is compatible with the loss of two water molecules per formula (theoretical  $9.8\%$ ). The difference between the observed and expected mass loss can be attributed to partial water loss during sample manipulation at room temperature.

The results of thermal dehydration observed for  $\text{K}_3[\text{Cr}(\text{CN})_5\text{NO}]\cdot 2\text{H}_2\text{O}$  is compatible with the X-ray structural analysis (Sect. 3.1) and spectroscopic results (Sect. 3.2.1) indicating that the two water molecules are un-equivalent to each other.

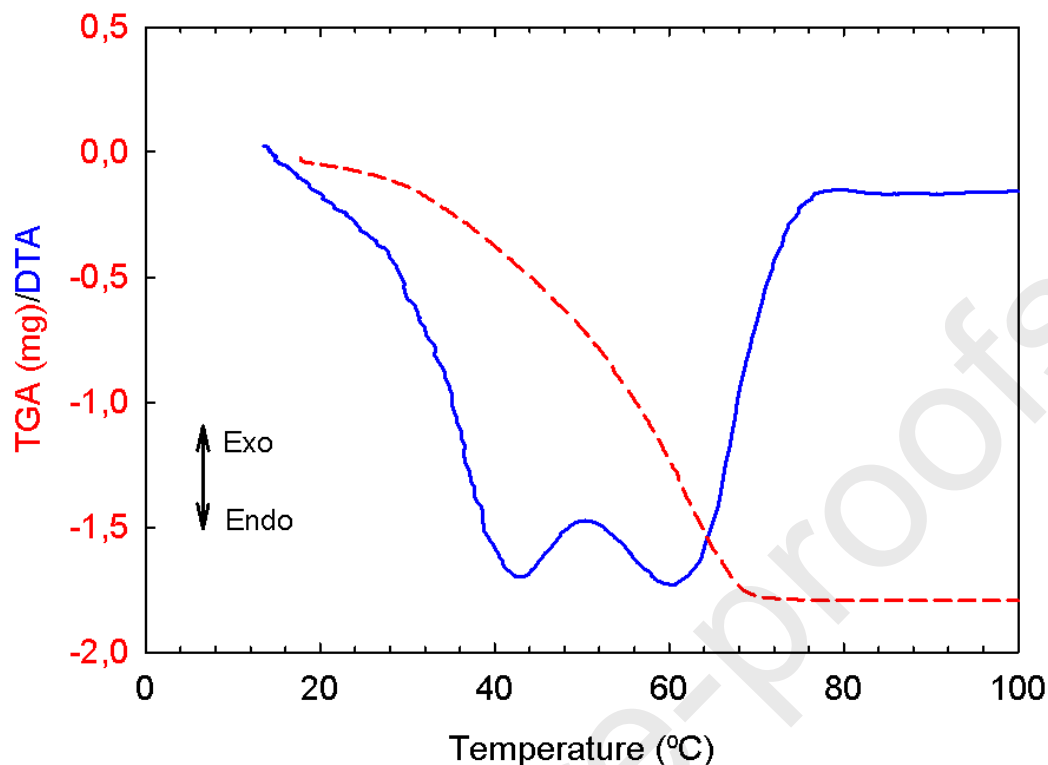


**Fig. 7.** TG (dashed red) and DT (solid blue) curves of  $K_3[Cr(CN)_5NO].2H_2O$  in the 15-100 °C temperature range (nitrogen atmosphere).

#### 4. Conclusions

After sixty years since it was first synthesized, by carefully controlling crystallization conditions and taking full advantage of modern X-ray diffraction data collection, advanced space group and structure solution and refinement, we report here precise bond distances and angles of  $[Cr^I(CN)_5NO]^{3-}$  complex in its hydrated potassium salt.

The complex crystallizes in space group  $Cc$  but shows pseudo-symmetry of super-group  $C2/c$  that renders the chromium ion on an impossible inversion centre and equivalent to each other two potassium ions and the water molecules. The chromium(I) complex is isomorphic to the manganese(I) analog,  $K_3[Mn(CN)_5NO].2H_2O$ .

The vibration structure of  $K_3[Cr(CN)_5NO].2H_2O$  was studied by IR and Raman spectroscopy and the assignment of modes assisted through comparison with the anhydrous complex and other first row transition metal analogs. Water vibration modes were detected in the IR spectra and fully identified and assigned employing deuterium-enriched samples.

Despite the crystallographic pseudo-symmetry relating to the two water molecules, TGA- DTA analysis clearly shows that these molecules are lost upon heating in two close but distinct steps at relatively low temperatures.

## Acknowledgments

We thank CONICET (Grants PIP 0651 and 0359), UNLP (Grants 11/X709, 11/X672 and 11/X831), and UNLu of Argentina for financial support. OEP, GAE and JAG are Research Fellows of CONICET.

## References.

- [1] S. E. Bari, J. A. Olabe, and L. D. Slep, “Three redox states of metallonitrosyls in aqueous solution,” in *Advances in Inorganic Chemistry*, vol. 67, Elsevier, 2015, pp. 87–144.
- [2] K. Belani, D. Hottinger, T. Kozhimannil, R. Prielipp, and D. Beebe, *J. Anaesthesiol. Clin. Pharmacol.* 30 (2014) 462–471. <https://doi.org/10.4103/0970-9185.142799>
- [3] D. M. P. Mingos, *Nitrosyl Complexes in Inorganic Chemistry, Biochemistry and Medicine I*. Oxford: Springer, 2014.
- [4] D. Schaniel and T. Woike, *Phys. Chem. Chem. Physics.*, 11 (2009) 4391–4395. <https://doi.org/10.1039/b900546c>
- [5] J. A. Guida, O. E. Piro, and P. J. Aymonino, *Solid State Commun.* 57 (1986) 175–178. [https://doi.org/10.1016/0038-1098\(86\)90133-X](https://doi.org/10.1016/0038-1098(86)90133-X)
- [6] J. H. Enemark, R. D. Feltham, *Coord. Chemo Rev.* 13 (1974) 339-406.
- [7] N. G. Vannerberg, *Acta Chem. Scand.* 20 (1966) 1571–1576.
- [8] J. H. Enemark, M. S. Quinby, L. L. Reed, M. J. Steuck, and K. K. Walthers, *Inorg. Chem.* 9 (1970) 2397–2403. <https://doi.org/10.1021/ic50093a003>
- [9] W. P. Griffith, J. Lewis and G. Wilkinson. *J. Chem. Soc.* (1959), 872–875. <https://doi.org/10.1039/JR9590000872>
- [10] “CrysAlisPro, Oxford Diffraction Ltd., version 1.171.33.48 (release 15-09-2009 CrysAlis171.NET).”
- [11] G. M. Sheldrick, *Acta Cryst. A* 71 (2015), 3–8. *Acta Cryst.* (2015). A71, 3-8 <https://doi.org/10.1107/S2053273314026370>

- [12] G. M. Sheldrick, *Acta Cryst*, A64 (2008) 112–122.  
<https://doi.org/10.1107/S0108767307043930>
- [13] H. D. Flack, *Acta Cryst*. A39 (1983) 876–88.  
<https://doi.org/10.1107/S0108767383001762>
- [14] R. O. Sheldrick, G. M.; Gould, *Acta Cryst*. B51 (1995) 423–431.
- [15] G. Burla, M. C.; Carrozzini, B.; Cascarano, G. L.; Giacovazzo, C.; Polidori, *J Appl Cryst*. 33 (2000) 307–311.
- [16] L. Palatinus.; A. van der Lee. *J Appl Cryst.*, 41 (2008) 975–984.  
<https://doi.org/10.1107/S0021889808028185>
- [17] L. J. Farrugia. *J Appl Cryst*. 30 (1997) 565–566.  
<https://doi.org/10.1107/S0021889897003117>
- [18] A. V. Tullberg, *Acta Chem Scand* 20 (1966) 1180–1180.  
<https://doi.org/10.3891/acta.chem.scand.20-1180>
- [19] N.-G. Tullberg, A.; Vannerberg, *Acta Chem Scand* 21 (1967) 1462–1472.
- [20] R.-J. Kou, H. -Z; Zhou, B. C.; Gao, S.; Liao, D. -Z; Wang *Inorg. Chem.*, 42 (2003) 5604–5611. <https://doi.org/10.1021/ic034028>
- [21] H. -Z. Ni, Z. -H.; Zheng, L.; Zhang, L. -F; Cui, A. -L; Ni, W. -W; Zhao, Ch. -Ch; Kou, *Eur.J.Inorg.Chem.* 46 (2007) 1240–1250.  
<https://doi.org/10.1002/ejic.200600958>
- [22] W.P. Griffith, *J. Chem. Soc.* (1963) 3286. [10.1039/JR9630003286](https://doi.org/10.1039/JR9630003286).
- [23] E. Miki, *Bull. Chem. Soc. Jpn.* 41 (1968) 1835–1844.  
<https://doi.org/10.1246/bcsj.41.1835>
- [24] K. Nakamoto, *Infrared and Raman Spectra of Inorganic and Coordination Compounds. Part A*, Sixth Edit. John Wiley & Sons, 2009.
- [25] M. Falk and O. Knop, *Water, a Comprehensive Treatise*. New York: Plenum Press, 1973.
- [26] D. B. Soria, J. I. Amalvy, and P. J. Aymonino *J. Crystallogr. Spectrosc. Res.* 17. (1987) 139–151.
- [27] O. Holzbecher, Michaela; Knop and M. Falk, *Can. J. Chem.* 49 (1971) 1413–1424.  
<https://doi.org/10.1139/v71-233>
- [28] K. Nakamoto, *Infrared and Raman Spectra of Inorganic and Coordination Compounds Part B: Applications in Coordination, Organometallic, and*

*Bioinorganic Chemistry*, 2009th ed. Hoboken, New Jersey: John Wiley & Sons, 2009.

- [29] J. A. Güida *Inorg. Chem. Commun.* 33 (2013) 75–77.  
<https://doi.org/10.1016/j.inoche.2013.03.022>
- [30] O. E. Piro, E. E. Castellano, J. A. Güida, and P. J. Aymonino, *Phys. Rev. B* 39 (1989) 1919–1926. <https://doi.org/10.1103/PhysRevB.39.1919>
- [31] L. Tosi, *Spectrochim. Acta Part A Mol. Spectrosc.* 29 (1973) 353–363.  
[https://doi.org/10.1016/0584-8539\(73\)80079-0](https://doi.org/10.1016/0584-8539(73)80079-0)
- [32] R. Rucki, “Sodium Nitroprusside,” in *Analytical Profiles of Drug Substances*, Elsevier, 1977, pp. 487–513. [https://doi.org/10.1016/S0099-5428\(08\)60352-4](https://doi.org/10.1016/S0099-5428(08)60352-4)
- [33] D. B. Soria, G. L. Estiu, R. E. Carbonio, and P. J. Aymonino *Spectrochim. Acta - Part A Mol. Biomol. Spectrosc.* 76 (2010) 270–275. doi:10.1016/j.saa.2010.03.034

**Table 1.**Crystal data and structure refinement results for  $K_3[Cr(CN)_5NO].2H_2O$ .

Empirical formula	$C_5H_4CrK_3N_6O_3$
Formula weight	365.44
Temperature	297(2) K
Wavelength	0.71073 Å
Crystal system	Monoclinic
Space group	$Cc$
Unit cell dimensions	$a = 17.8379(6)$ Å $b = 7.1589(2)$ Å $c = 11.5293(4)$ Å $\beta = 118.005(5)^\circ$
Volume	$1299.89(9)$ Å <sup>3</sup>
Z, density (calculated)	4, 1.867 Mg/m <sup>3</sup>
Absorption coefficient	$1.848$ mm <sup>-1</sup>
F(000)	724
Crystal size	$0.188 \times 0.136 \times 0.113$ mm <sup>3</sup>
$\vartheta$ -range for data collection	$3.126$ to $28.801^\circ$ .
Index ranges	$-23 \leq h \leq 23$ , $-9 \leq k \leq 8$ , $-12 \leq l \leq 15$
Reflections collected	4981
Independent reflections	2380 [R(int) = 0.0214]
Observed reflections [I>2 $\sigma$ (I)]	2251
Completeness to $\vartheta = 25.242^\circ$	99.9 %
Refinement method	Full-matrix least-squares on F <sup>2</sup>
Data / restraints / parameters	2380 / 8 / 180
Goodness-of-fit on F <sup>2</sup>	1.080
Final R indices <sup>a</sup> [I>2 $\sigma$ (I)]	R1 = 0.0274, wR2 = 0.0644
R indices (all data)	R1 = 0.0299, wR2 = 0.0671
Absolute structure parameter	0.26(3)
Largest diff. peak and hole	0.234 and -0.537 e.Å <sup>-3</sup>

<sup>a</sup> $R_1 = \sum ||F_o| - |F_c|| / \sum |F_o|$ ,  $wR_2 = [\sum w(|F_o|^2 - |F_c|^2)^2 / \sum w(|F_o|^2)^2]^{1/2}$

**Table 2.**

Candidate space groups with the best figures of merit obtained with SHELXT[10] from the centre-symmetric and two noncentre-symmetric monoclinic space subgroups with the Laue group  $C2/m$  ( $C_{2h}$ ) of  $K_3[Cr(CN)_5NO].2H_2O$ . The table also includes the corresponding chemical formula derived from the integrated electron density around the peaks of the maps.

S.G.	R1	R(weak)	$\alpha$	Flack's x	Formula
$C2/c$	0.148	0.187	0.073		$C_6N_2O_6K_3Cr$
$Cc$	0.089	0.027	0.008	0.27	$C_6N_2O_6K_3Cr$
$C2$	0.141	0.022	0.101	0.48	$C_6N_2O_6K_3Cr$

**Table 3.**

Bond lengths [ $\text{\AA}$ ] and angles [ $^\circ$ ] within the  $[Cr(CN)_5NO]^{3-}$  complex in  $K_3[Cr(CN)_5NO].2H_2O$ .

Cr-N(1)	1.699(3)	C(2)-Cr-C(4)	171.6(2)
Cr-C(2)	2.062(4)	C(5)-Cr-C(4)	89.6(2)
Cr-C(5)	2.065(5)	N(1)-Cr-C(6)	91.2(2)
Cr-C(4)	2.068(4)	C(2)-Cr-C(6)	89.7(2)
Cr-C(6)	2.072(4)	C(5)-Cr-C(6)	170.8(2)
Cr-C(3)	2.100(4)	C(4)-Cr-C(6)	90.0(2)
N(1)-O(1)	1.209(4)	N(1)-Cr-C(3)	177.8(2)
C(2)-N(2)	1.151(6)	C(2)-Cr-C(3)	88.9(2)
C(3)-N(3)	1.147(5)	C(5)-Cr-C(3)	83.9(2)
C(4)-N(4)	1.148(6)	C(4)-Cr-C(3)	82.8(2)
C(5)-N(5)	1.148(6)	C(6)-Cr-C(3)	86.9(2)
C(6)-N(6)	1.145(7)	O(1)-N(1)-Cr	174.3(3)
		N(2)-C(2)-Cr	174.5(4)
N(1)-Cr-C(2)	90.1(2)	N(3)-C(3)-Cr	173.5(4)
N(1)-Cr-C(5)	98.0(2)	N(4)-C(4)-Cr	176.2(4)
C(2)-Cr-C(5)	89.3(2)	N(5)-C(5)-Cr	178.1(5)
N(1)-Cr-C(4)	98.2(2)	N(6)-C(6)-Cr	177.6(4)

**Table 4.**Short contacts[Å] around potassium ions in  $K_3[Cr(CN)_5NO].2H_2O$  (up to 3.35Å)

K(1)-N(3)	2.801(4)	K(2)-O(1W)	2.803(4)	K(3)-O(2W)	2.787(4)
K(1)-O(1)#1	2.829(4)	K(2)-N(6)#4	2.850(5)	K(3)-N(5)#9	2.873(5)
K(1)-N(2)#2	2.978(5)	K(2)-O(2W)#5	2.876(4)	K(3)-O(1W)#10	2.884(4)
K(1)-N(4)#3	2.999(5)	K(2)-O(1)#6	3.021(3)	K(3)-N(3)#11	2.936(3)
		K(2)-N(3)#7	3.031(4)	K(3)-N(6)#2	3.159(5)
		K(2)-N(4)#7	3.110(4)	K(3)-N(4)#2	3.171(5)
		K(2)-N(2)#8	3.124(5)	K(3)-O(1)#12	3.185(3)
		K(2)-O(2W)#7	3.261(4)	K(3)-N(2)#12	3.206(4)
		K(2)-N(5)#8	3.321(6)	K(3)-O(1W)#12	3.263(4)

Symmetry transformations used to generate equivalent atoms:

(#1)  $x, -y+1, z-1/2$ ; (#2)  $x, y+1, z$ ; (#3)  $x, -y+2, z-1/2$ ; (#4)  $x-1/2, -y-1/2, z-1/2$ ; (#5)  $x-1/2, y-3/2, z-1$ ;  
 (#6)  $x, -y, z-1/2$ ; (#7)  $x-1/2, -y+1/2, z-1/2$ ; (#8)  $x, y-1, z$ ; (#9)  $x+1/2, -y+5/2, z+1/2$ ; (#10)  $x+1/2, y+3/2, z+1$ ;  
 (#11)  $x, -y+2, z+1/2$ ; (#12)  $x+1/2, -y+3/2, z+1/2$ .

**Table 5.**Hydrogen bond distances [Å] and angles [°] for  $K_3[Cr(CN)_5NO].2H_2O$ .

D-H...A	d(D-H)	d(H...A)	d(D...A)	∠(DHA)
O(2W)-H(2A)...N(4)	0.85(1)	2.01(2)	2.851(5)	169(4)
O(1W)-H(1A)...N(2)	0.86(1)	2.01(2)	2.870(5)	172(5)
O(1W)-H(1B)...N(6)#1	0.86(1)	2.69(4)	3.310(6)	130(4)
O(2W)-H(2B)...N(1)#2	0.86(1)	2.65(4)	3.101(5)	114(4)
O(2W)-H(2B)...N(5)#2	0.86(1)	2.61(3)	3.391(6)	152(4)

Symmetry transformations used to generate equivalent atoms: (#1)  $x-1/2, -y+1/2, z-1/2$ ;(#2)  $x+1/2, -y+3/2, z+1/2$ .



**Table 6.**

Infrared frequencies ( $\text{cm}^{-1}$ ) for water and partially deuterated samples for polycrystalline  $\text{K}_3[\text{Cr}(\text{CN})_5\text{NO}]\cdot 2\text{H}_2\text{O}$  measured at  $10^\circ\text{C}$ .

$\text{K}_3[\text{Cr}(\text{CN})_5\text{NO}]\cdot 2\text{H}_2\text{O}$	HOD	$\text{D}_2\text{O}$	Water mode
3592	2656		$\nu_{\text{as}}(\nu_3)$
	2641w		isolated
3392	2500		$\nu_{\text{sim}}(\nu_1)$
3289			} $2\delta(\text{H}_2\text{O})$
3255			
		2396	$2\delta(\text{D}_2\text{O})$
1646	1460		} $\delta(\nu_2)$
	1425	1209	
1630	1411	1197	
661			} L( $\text{H}_2\text{O}$ )
490(sh)broad			
455broad			
414(sh)	415(sh)		
387(sh)	388(sh)		
	355(sh)		
	324		

**Table 7.**

Assignments of bands in the IR and Raman spectra of pentacyanonitrosylchromate(I) dihydrate and anhydrous.

$K_3[Cr(CN)_5NO] \cdot 2H_2O$		$K_3[Cr(CN)_5NO]$		Assignment
Infrared	Raman	Infrared	Raman	
3592				$\nu(OH)_{as.}$
3392				$\nu(OH)_{sim}$
3252		3265		$2\nu(NO)$
		3234		
2125	2125	2127(h)	2127	$\nu(CN)_{ax}$
2117	2119(sh)	2120	2120(sh)	$\nu(CN)_{eq}$
2112				$\nu(CN)_{eq}$
		2094	2094	
2077	2077	2078	2078	$\nu(^{13}CN)$
1658		1643		$\nu(NO)$
		1629(sh)		
1646				$\delta(HOH)$
1630				
661				L(H <sub>2</sub> O)
627	629	622	622	$\nu(CrN)$
619	615	614	622	$\delta(CrNO)$
490				L(H <sub>2</sub> O)
455				L(H <sub>2</sub> O)
438	440	431	430	$\nu(CrC)$
414(h)				L(H <sub>2</sub> O)
	418		421	and
399	398	400	390	$\delta(CrCN)$
	358	357(h)		
349	346	348	350	
297		291		
	206			
	180(h)			
	163(h)		179	
	151			
			159	
	127		117	
	108		101	

**Highlights**

- Accurate metrics of  $[\text{Cr}^{\text{I}}(\text{CN})_5\text{NO}]^{3-}$  complex in its dihydrate potassium salt
- Advanced X-ray data collection and space group and structure solution and refinement
- $\text{K}_3[\text{Cr}(\text{CN})_5\text{NO}]\cdot 2\text{H}_2\text{O}$  isomorphous to the Mn(I) analogue
- IR and Raman spectra with assignment of water modes assisted by deuterium-enrichment

Professor Jens Müller

Editor

Inorganica Chimica Acta

Münster, Germany

Your reference Ms.ID: ICA\_2020\_391

Dear Professor Müller

Please find submitted on-line the new version of our manuscript, which was revised taking into account the many helpful comments and suggestions from the Referees.

For convenience, I shall detail the corrections and answers to the points raised by the Reviewers, following the pattern of your decision letter. Our replies, modifications and aggregates to the original manuscript are emphasized by light blue coloured text.

I trust that the revised manuscript will now meet your approval for publication and look forward to your reply.

With my best regards,

Dr. Jorge A. Güida